AFCRL-72-0282
23 MARCH 1972
PHYSICAL SCIENCES RESEARCH PAPERS, NO. 483

AIR FORCE CAMBRIDGE RESEARCH LABORATORIES
L. G. HANSCOM FIELD, BEDFORD, MASSACHUSETTS

Thermal Lensing in Infrared Laser Window Materials

P.D. GIANINO
J.R. JASPERSE

AIR FORCE SYSTEMS COMMAND
United States Air Force

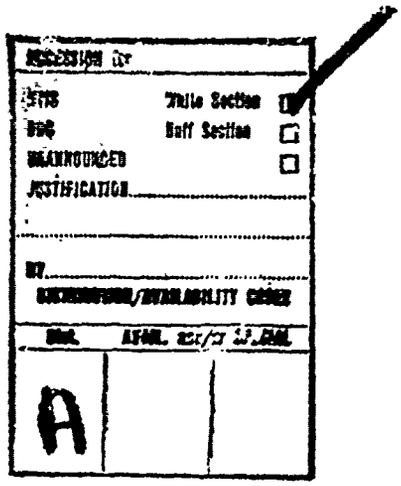

Qualified requestors may obtain additional copies from the Defense Documentation Center. All others should apply to the National Technical Information Service.

Unclassified

Security Classification

DOCUMENT CONTROL DATA - R&D

(Security classification of title, body of abstract and indexing annotation must be entered when the overall report is classified)

1. ORIGINATING ACTIVITY *(Corporate author)*
Air Force Cambridge Research Laboratories (LQR)
L. G. Hanscom Field
Bedford, Massachusetts 01730

2a. REPORT SECURITY CLASSIFICATION
Unclassified

2b. GROUP

3. REPORT TITLE

THERMAL LENSING IN INFRARED LASER WINDOW MATERIALS

4. DESCRIPTIVE NOTES *(Type of report and inclusive dates)*
Scientific. Interim.

5. AUTHOR(S) *(First name, middle initial, last name)*
P. D. Gianino
J. R. Jasperse

6. REPORT DATE	7a. TOTAL NO. OF PAGES	7b. NO. OF REFS
23 March 1972	51	16

8a. CONTRACT OR GRANT NO.	9a. ORIGINATOR'S REPORT NUMBER(S)
b. PROJECT, TASK, WORK UNIT NOS. 3326-05-01	AFCRL-72-0202
c. DOD ELEMENT 62601F	9b. OTHER REPORT NO(S) *(Any other numbers that may be assigned this report)*
d. DOD SUBELEMENT S662300	PSRP, No. 483

10. DISTRIBUTION STATEMENT

Approved for public release; distribution unlimited.

11. SUPPLEMENTARY NOTES	12. SPONSORING MILITARY ACTIVITY
This research was supported by the Air Force Weapons Laboratory, Kirtland Air Force Base, Albuquerque, New Mexico	Air Force Cambridge Research Laboratories (LQR) L. G. Hanscom Field Bedford, Massachusetts 01730

13. ABSTRACT

A theoretical investigation of thermal lensing in infrared windows is presented which treats aberration effects to all orders in the small angle-of-deviation approximation. The model is applied to a truncated, Gaussian, infrared laser beam incident on a semitransparent, isotropic, disc-shaped window. It is shown that window aberrations limit the time a diffraction-limited focus can be held in the far-field. This diffraction-limited time t_d is computed for some candidate window materials and their relative merits are discussed. Some approaches to solving the thermal lensing problem from both an engineering and a materials point of view, as well as some program research and development needs, are discussed.

DD FORM 1 NOV 65 1473

Unclassified

Security Classification

14. KEY WORDS	LINK A		LINK B		LINK C	
	ROLE	WT	ROLE	WT	ROLE	WT
Thermal lensing in solids						
IR Window						
IR Window Materials						
Laser Window						
Laser Window Materials						
Diffraction-limited time						

ih

AFCRL-72-0202
23 MARCH 1972
PHYSICAL SCIENCES RESEARCH PAPERS, NO. 483

SOLID STATE SCIENCES LABORATORY PROJECT 3326

AIR FORCE CAMBRIDGE RESEARCH LABORATORIES
L. G. HANSCOM FIELD, BEDFORD, MASSACHUSETTS

Thermal Lensing in Infrared Laser Window Materials

P.D. GIANINO
J.R. JASPERSE

AIR FORCE SYSTEMS COMMAND
United States Air Force

Abstract

A theoretical investigation of thermal lensing in infrared windows is presented which treats aberration effects to all orders in the small angle-of-deviation approximation. The model is applied to a truncated, Gaussian, infrared laser beam incident on a semitransparent, isotropic, disc-shaped window. It is shown that window aberrations limit the time a diffraction-limited focus can be held in the far-field. This diffraction-limited time t_d is computed for some candidate window materials and their relative merits are discussed. Some approaches to solving the thermal lensing problem from both an engineering and a materials point of view, as well as some program research and development needs, are discussed.

Contents

Contents

Illustrations

Tables

Thermal Lensing in Infrared Laser Window Materials

1. INTRODUCTION

Recent advances in high-power infrared lasers (Emmett, 1971) suggest the possibility of focusing large power densities in the far-field. If, however, a laser beam of nonuniform intensity passes through a semitransparent window the beam will be distorted as the window heats up.

Distortion of a laser beam passing through a liquid cell has been observed and attributed (Gordon et al, 1965; Tien et al, 1965) to a lensing action in the liquid caused by nonuniform heating. Theoretical treatments of some problems quite close to the one examined in this paper have also been given (Tien et al, 1965; Quelle, 1966; Foster et al, 1970). In fact, Sparks (1971) showed that a significant amount of thermal lensing will occur in an infrared window well before it fails due to other causes. For a discussion of other modes of failure see Horrigan et al (1969). These treatments have been restricted to a parabolic dependence of the index of refraction with position, hence, no aberration of the beam occurs. Ring-like interference patterns have been observed, however, and attributed to aberration effects produced by thermal lensing in low-loss liquids (Whinnery et al, 1967).

In this paper we extend previous treatments of thermal lensing (Quelle, 1966; Foster et al, 1970; Sparks, 1971) to include window aberrations to all orders and

(Received for publication 23 March 1972)

we apply the analysis to the specific problem of calculating the amount of time the far-field focused spot remains diffraction-limited (Jasperse et al, 1972). This diffraction-limited time t_d, turns out to be independent of the beam radius, the distance from the window to the spot, and the Gaussian focal lengths of the window. Our analysis provides the laser systems engineer with one criterion for choosing among candidate windows and also suggests to the materials engineer several possibilities for designing new materials.

2. A SOLVABLE MODEL FOR THERMAL LENSING IN ISOTROPIC, DISC-SHAPED WINDOWS

2.1 Outline of the Calculation

In this section we generalize previous treatments of thermal lensing of a TEM_{oo} laser beam to include all orders of aberration produced by a time-dependent temperature distribution in an isotropic, disc-shaped exit window. Employing cylindrical coordinates (ρ, ϕ, z) we assume that the temperature distribution so generated is independent of ϕ. Furthermore, we assume a small angle of deviation for a normally incident ray, allowing us to neglect the temperature's dependence on z since it will have a negligible effect on the bending of the ray. This means that, in effect, we are dealing with a lens system which has a long but finite focal length. The total angular deviation θ_w, of any ray in such a window, is the sum of two parts:

$$\theta_w = \theta_{\text{grad n}} + \theta_{\text{bulge}} , \tag{1}$$

where $\theta_{\text{grad n}}$ is the contribution due to a gradient in the refractive index n, and θ_{bulge} is the contribution due to a bulging of the originally parallel faces of the window. Such an equation holds for both the ρ- and ϕ-polarized rays.

2.2 Calculation of n

We consider a temperature distribution in the window having the following particular form when expressed in cylindrical coordinates:

$$T(\rho/\rho_o, t) = T(0,0) + g(t)\, T(\rho/\rho_o) , \tag{2}$$

where T(0, 0) is a constant, g(t) is any function of time, ρ is the radial coordinate, and ρ_o is the window radius. The term $T(\rho/\rho_o)$ is any monotonically increasing or decreasing even function of ρ expressible as the following convergent power series in ρ/ρ_o:

$$T(\rho/\rho_o) = \sum_{\ell=0}^{\infty} T_{2\ell} \, (\rho/\rho_o)^{2\ell} \, . \tag{3}$$

The $T_{2\ell}$ are dimensionless constants, with $T_o = 1$.

A fundamental theory accurately establishing the index n, in terms of frequency, temperature, and positions of all ions or atoms within the solid, is not available. In place of such a theory, we develop a phenomenological treatment of thermal lensing by regarding n at a given frequency as a function of temperature and the appropriate strain tensor components. For the case of a plane stress in a disc of isotropic material, the only nonvanishing strain components in cylindrical coordinates are $\epsilon_{\rho\rho}$, $\epsilon_{\phi\phi}$, and ϵ_{zz} . Thus, in our case, the refractive index may be determined by specifying the values of three quantities n_i, i representing ρ, ϕ, and z, where

$$n_i = n_i \, (T, \, \epsilon_{\rho\rho}, \, \epsilon_{\phi\phi}, \, \epsilon_{zz}) \, . \tag{4}$$

For a fixed time, the temperature and the strains depend only on ρ. Therefore, for a small change in n_i, and following the development given by Quelle (1966) and Sparks (1971) we write:

$$\Delta n_i = \left(\frac{\partial n_i}{\partial T}\right) \Delta T + \left(\frac{\partial n_i}{\partial \epsilon_{\rho\rho}}\right) \Delta \epsilon_{\rho\rho}$$

$$+ \left(\frac{\partial n_i}{\partial \epsilon_{\phi\phi}}\right) \Delta \epsilon_{\phi\phi} + \left(\frac{\partial n_i}{\partial \epsilon_{zz}}\right) \Delta \epsilon_{zz} \, . \tag{5}$$

In matrix form, these equations become:

$$\begin{pmatrix} \Delta n_\rho \\ \Delta n_\phi \\ \Delta n_z \end{pmatrix} = \begin{pmatrix} \partial n_\rho/\partial T \\ \partial n_\phi/\partial T \\ \partial n_z/\partial T \end{pmatrix} \Delta T + J \left(\frac{n_\rho, \, n_\phi, \, n_z}{\epsilon_{\rho\rho}, \, \epsilon_{\phi\phi}, \, \epsilon_{zz}} \right) \begin{pmatrix} \Delta \epsilon_{\rho\rho} \\ \Delta \epsilon_{\phi\phi} \\ \Delta \epsilon_{zz} \end{pmatrix} \, , \tag{6}$$

in which n_ρ, n_ϕ, and n_z are the components of refractive index along the three orthogonal directions, and $J(n_\rho, n_\phi, n_z/\epsilon_{\rho\rho}, \epsilon_{\phi\phi}, \epsilon_{zz})$ is the "Jacobian-like" matrix of the transformation between the n_i and the ϵ_{jj}, defined as:

$$\begin{pmatrix} \frac{\partial n_\rho}{\partial \epsilon_{\rho\rho}} & \frac{\partial n_\rho}{\partial \epsilon_{\phi\psi}} & \frac{\partial n_\rho}{\partial \epsilon_{zz}} \\ \frac{\partial n_\phi}{\partial \epsilon_{\rho\rho}} & \frac{\partial n_\phi}{\partial \epsilon_{\phi\phi}} & \frac{\partial n_\phi}{\partial \epsilon_{zz}} \\ \frac{\partial n_z}{\partial \epsilon_{\rho\rho}} & \frac{\partial n_z}{\partial \epsilon_{\phi\phi}} & \frac{\partial n_z}{\partial \epsilon_{zz}} \end{pmatrix} .$$

In an isotropic disc under plane stress and at a fixed temperature the Pockels elasto-optic constants p_{ij}, also called the strain-optic coefficients, are defined by (Krishnan, 1958):

$$\begin{pmatrix} \frac{1}{n_\rho^2} - \frac{1}{n_o^2} \\ \frac{1}{n_\phi^2} - \frac{1}{n_o^2} \\ \frac{1}{n_z^2} - \frac{1}{n_o^2} \end{pmatrix} = \begin{pmatrix} p_{11} & p_{12} & p_{12} \\ p_{12} & p_{11} & p_{12} \\ p_{12} & p_{12} & p_{11} \end{pmatrix} \begin{pmatrix} \epsilon_{\rho\rho} \\ \epsilon_{\phi\phi} \\ \epsilon_{zz} \end{pmatrix} , \qquad (7)$$

n_o being the unstrained refractive index. Under the conditions when the n_i are not too much different than n_o, each element on the left-hand side of Eq. (7) can be approximated by $-2(n_i-n_o)/n_o^3$. This allows Eq. (7) to be rewritten as:

$$\begin{pmatrix} n_\rho - n_o \\ n_\phi - n_o \\ n_z - n_o \end{pmatrix} = \frac{-n_o^3}{2} \begin{pmatrix} p_{11} & p_{12} & p_{12} \\ p_{12} & p_{11} & p_{12} \\ p_{12} & p_{12} & p_{11} \end{pmatrix} \begin{pmatrix} \epsilon_{\rho\rho} \\ \epsilon_{\phi\phi} \\ \epsilon_{zz} \end{pmatrix} . \qquad (8)$$

With the aid of Eqs. (8), one can calculate each $\partial n_i/\partial \epsilon_{jj}$ so that the J-matrix in Eq. (6) can be replaced by:

$$J\left(\frac{n_\rho, n_\phi, n_z}{\epsilon_{\rho\rho}, \epsilon_{\phi\phi}, \epsilon_{zz}}\right) = -\frac{n_c^3}{2}\begin{pmatrix} p_{11} & p_{12} & p_{12} \\ p_{12} & p_{11} & p_{12} \\ p_{12} & p_{12} & p_{11} \end{pmatrix} . \qquad (9)$$

The thermally induced stress-strain relations are (Boley et al, 1960):

$$\begin{pmatrix} \epsilon_{\rho\rho} \\ \epsilon_{\phi\phi} \\ \epsilon_{zz} \end{pmatrix} = \frac{1}{Y}\begin{pmatrix} 1 & -\nu & -\nu \\ -\nu & 1 & -\nu \\ -\nu & -\nu & 1 \end{pmatrix}\begin{pmatrix} \sigma_{\rho\rho} \\ \sigma_{\phi\phi} \\ \sigma_{zz} \end{pmatrix} + \alpha T\begin{pmatrix} 1 \\ 1 \\ 1 \end{pmatrix} , \qquad (10)$$

where Y is Young's modulus, the σ_{ii} are the three stress components in cylindrical coordinates, ν is Poisson's ratio, and α is the linear expansion coefficient. Now we can define the initially unstrained "fiducial state" as that for which all σ_{jj} are zero at zero time and at the uniform temperature T(0, 0). Then, any change in temperature and/or stresses produces the following change in strains:

$$\begin{pmatrix} \Delta\epsilon_{\rho\rho} \\ \Delta\epsilon_{\phi\phi} \\ \Delta\epsilon_{zz} \end{pmatrix} = \frac{1}{Y}\begin{pmatrix} 1 & -\nu & -\nu \\ -\nu & 1 & -\nu \\ -\nu & -\nu & 1 \end{pmatrix}\begin{pmatrix} \sigma_{\rho\rho} \\ \sigma_{\phi\phi} \\ \sigma_{zz} \end{pmatrix} + \alpha \Delta T\begin{pmatrix} 1 \\ 1 \\ 1 \end{pmatrix} . \qquad (11)$$

From Eqs. (6) note that each $\partial n_i/\partial T$ is measured at constant strain. Since each n_i is not too much different from n_o, there would be no loss in generality if each $\partial n_i/\partial T$ were replaced by the derivative evaluated in the fiducial condition, namely, $[\partial n/\partial T]_{n\approx n_o}$. Substituting this information, together with Eqs. (9) and (11), into (6), and, using the fact that the Δn_i can also be expressed as $(n_i - n_o)$, we get after simplifying:

$$\begin{pmatrix} n_\rho - n \\ n_\phi - n \\ n_z - n \end{pmatrix} = \left(\frac{\partial n}{\partial T}\right)_{\sigma=0} \Delta T \begin{pmatrix} 1 \\ 1 \\ 1 \end{pmatrix} - \frac{n^3}{2Y} \begin{pmatrix} C_o & C_1 & C_1 \\ C_1 & C_o & C_1 \\ C_1 & C_1 & C_o \end{pmatrix} \begin{pmatrix} \sigma_{\rho\rho} \\ \sigma_{\phi\phi} \\ \sigma_{zz} \end{pmatrix}, \tag{12}$$

where

$$\left(\frac{\partial n}{\partial T}\right)_{\sigma=0} \equiv \left(\frac{\partial n_o}{\partial T}\right)_{\epsilon=0} - \frac{\alpha n_o^3}{2} \left(p_{11} + 2p_{12}\right), \tag{13}$$

with n denoting the average index of refraction,

$$C_o \equiv p_{11} - 2\nu p_{12}, \tag{14}$$

$$C_1 \equiv (1-\nu)\, p_{12} - \nu p_{11}, \tag{15}$$

and

$$\Delta T \equiv T(\rho/\rho_o, t) - T(0,0). \tag{16}$$

The C's are related to the parallel and normal components of the stress-optic coefficients ($B_\parallel$ and $B_\perp$, respectively) via:

$$B_\parallel = \frac{n^3}{2Y} C_o \tag{17}$$

and

$$B_\perp = \frac{n^3}{2Y} C_1. \tag{18}$$

For plane stresses in isotropic materials with disc-type geometry, the relationship between the stress and the temperature change from the fiducial state is (Boley et al, 1960):

$$\sigma_{\rho\rho} = \alpha Y \left\{ \int_0^1 dx\, x\, \Delta T(x,t) - (\rho_0/\rho)^2 \int_0^{\rho/\rho_0} dx\, x\, \Delta T(x,t) \right\}, \tag{19a}$$

$$\sigma_{\phi\phi} = \alpha Y \left\{ \int_0^1 dx\, x\, \Delta T(x,t) + (\rho_0/\rho)^2 \int_0^{\rho/\rho_0} dx\, x\, \Delta T(x,t) - \Delta T(\rho/\rho_0, t) \right\}, \tag{19b}$$

$$\sigma_{zz} = 0 .$$

Using Eqs. (16) and (3) for $\Delta T(\rho/\rho_0, t)$ in Eqs. (19), inserting these results for the σ_{ii} into Eqs. (12), and solving for each n_i results in:

$$n_\rho(\rho/\rho_0, t) = n_\rho(0,t) + g(t) \sum_{\ell=1}^{\infty} n_{2\ell}^{\rho} (\rho/\rho_0)^{2\ell} , \tag{20a}$$

$$n_\phi(\rho/\rho_0, t) = n_\phi(0,t) + g(t) \sum_{\ell=1}^{\infty} n_{2\ell}^{\phi} (\rho/\rho_0)^{2\ell} . \tag{20b}$$

The quantities $n_\rho(0,t)$ and $n_\phi(0,t)$ specify the tir e dependence of the index of refraction at the center of the window, while the $n_{\cdot\cdot}$ and the $n_{2\ell}^{\phi}$ are given by:

$$n_{2\ell}^{\rho} \equiv T_{2\ell} \left\{ \left(\frac{\partial n}{\partial T}\right)_{\sigma=0} + \frac{\alpha n^3}{2(2\ell+2)} \left[(1-(2\ell+1)\nu)p_{11} + (2\ell+1-(2\ell+3)\nu)p_{12} \right] \right\}, \tag{21a}$$

$$n_{2\ell}^{\phi} \equiv T_{2\ell} \left\{ \left(\frac{\partial n}{\partial T}\right)_{\sigma=0} + \frac{\alpha n^3}{2(2\ell+2)} \left[(2\ell+1-\nu)p_{11} + (1-(4\ell+3)\nu)p_{12} \right] \right\}. \tag{21b}$$

The details of this derivation are given in Appendix A.

The equation for n_z is not written out since its effect on the bending of a ray in the small angle-of-deviation approximation is negligible.

The fact that the indices of refraction are different for each polarization shows that the window develops a stress-induced birefringence.

2.3 Calculation of $\theta_{\text{grad n}}$

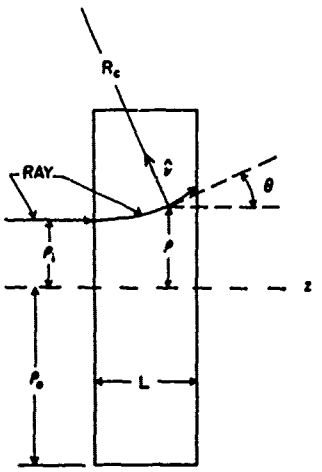

Figure 1. The Bending of a Ray as It Passes Through a Disc-Shaped Window

Consider a ray normally incident at a distance ρ_i from the z axis of a parallel-faced disc, having an index $n(\rho/\rho_o, t)$ as shown in Figure 1. A nonlinear, second-order, differential equation for the ray's trajectory (ρ as a function of z) in the small angle-of-deviation approximation is solved approximately in Appendix B. Its solution is:

$$\rho \cong \rho_i \left[1+Kz^2 + O\left\{|K|^2 z^4\right\}\right], \tag{22}$$

where

$$K \equiv \left(\frac{g(t)}{n(0,t)\rho_o\rho_i}\right) \sum_{\ell=1}^{\infty} n_{2,\ell} (\rho_i/\rho_o)^{2\ell-1} . \tag{23}$$

Applying Snell's Law at the exit surface of the window, we see that:

$$n(0,t) \cong \left.\frac{\text{refracted angle}}{\text{incident angle}}\right|_{z=L_o} \cong \left.\frac{\theta_{\text{grad n}}}{[d\rho/dz]}\right|_{z=L_o} , \tag{24}$$

where L_o is the initial thickness of the window. From Eq. (22), including up to second order:

$$\left.\frac{d\rho}{dz}\right|_{z=L_o} = 2\,\rho_i\,K\,L_o . \tag{25}$$

Utilizing Eqs. (23) and (25) in (24), we obtain a stress-induced birefringence in $\theta_{\text{grad n}}$ given for ρ and ϕ polarizations by:

$$\theta^{\rho}_{\text{grad n}} = 2\rho_i L_o\, n(0,t)\, K^{\rho} = \frac{2L_o g(t)}{\rho_o} \sum_{\ell=1}^{\infty} n^{\rho}_{2\ell}\, \ell \left(\frac{\rho_i}{\rho_o}\right)^{2\ell-1} , \tag{26a}$$

$$\theta^{\phi}_{\text{grad n}} = 2\rho_i L_o\, n(0,t)\, K^{\phi} = \frac{2L_o g(t)}{\rho_o} \sum_{\ell=1}^{\infty} n^{\phi}_{2\ell}\, \ell \left(\frac{\rho_i}{\rho_o}\right)^{2\ell-1} . \tag{26b}$$

Throughout this paper we adopt the convention that the angle that any deviated ray makes with the horizontal will be positive if the ray bends away from the z axis and negative if towards the z axis.

2.4 Calculation of θ_{bulge}

The equation for the plane curve L associated with one face of the bulging window is:

$$L(\rho/\rho_o, t) = L_o + \frac{1}{2} L_o\, \Delta\, \epsilon_{zz} . \tag{27}$$

Utilizing Eqs. (11) for $\Delta\epsilon_{zz}$, Eqs. (A-4) and (A-5) for $\sigma_{\rho\rho}$ and $\sigma_{\phi\phi}$, and Eq. (A-1) for ΔT, the above equation can be rewritten as:

$$L(\rho/\rho_o, t) = L(0,t) + \frac{L_o g(t)\, \alpha\, (1+\nu)}{2} \sum_{\ell=1}^{\infty} T_{2\ell}\, (\rho/\rho_o)^{2\ell} \tag{28}$$

in which, as usual, all the terms independent of ρ have been collected under the symbol L (0, t). In Appendix C, we show that θ_{bulge} can be expressed as:

$$\theta_{\text{bulge}} = 2(n-1)\left(\frac{dL}{d\rho}\right)_{\rho=\rho_i} . \tag{29}$$

Utilizing Eq. (28) results in:

$$\theta_{\text{bulge}} = \left(\frac{2L_o g(t)}{\rho_o}\right) \alpha\, (1+\nu)(n-1) \sum_{\ell=1}^{\infty} T_{2\ell}\, \ell\, (\rho_i/\rho_o)^{2\ell-1} . \tag{30}$$

2.5 The Window Angle of Deviation, θ_w

The total angle of deviation due to the window itself, θ_w^j, (where j can stand for either ρ or ϕ polarizations) can be obtained by inserting Eqs. (26 a or b) and (30) into (1). It is *

$$\theta_w^j = \left(\frac{2\,L_o g(t)}{\rho_o}\right) \sum_{\ell=1}^{\infty} \ell \left\{ n_{2\ell}^j + \alpha\,(1+\nu)(n-1)\,T_{2\ell} \right\} \left(\frac{\rho_i}{\rho_o}\right)^{2\ell-1} . \tag{31}$$

The Gaussian focal lengths R_G^j are related to the terms of θ_w^j, which are linear in ρ_i. They are

$$R_G^j \cong \frac{\rho_i}{\theta_w^j} = \frac{\rho_o^2}{2\,L_o g(t)\left\{ n_2^j + \alpha\,(1+\nu)(n-1)\,T_2 \right\}} . \tag{32}$$

We note that all formulas in Section 2 apply for both transient and steady-state conditions, since g(t) may be any function of time.

3. APPLICATION TO A TRUNCATED GAUSSIAN LASER BEAM INCIDENT ON A DISC-SHAPED, ISOTROPIC WINDOW

3.1 Assumptions

In applying the solvable model given in Section 2 to the specific problem of a laser pulse** of time t incident on a semitransparent, disc-shaped window, we make the following assumptions:

(1) total angular deviations are less than about 10^{-2} radians;

(2) the window material is isotropic;

(3) the thermally induced stresses and the corresponding strains are perfectly elastic;

---

* The first two terms of each of these series have also been derived by a Raytheon group using a different method, namely, by computing phase differences between rays traversing the window at different radial distances. Their phase angles are related to our θ_w^j via $\int_o^\rho k\,\theta_w^j\,d\rho$. See F.A. Horrigan and T.F. Deutsch, Raytheon Research Division, Second Quarterly Report, Contract No. DAAH01-70-C-1251 (1970).

** The mode of laser operation contemplated here is interrupted cw with typical values of t on the order of a few seconds.

(4) the laser pulse time is less than or comparable to the smallest of the characteristic times for heat flow;

(5) bulk absorption dominates other loss mechanisms in the calculation of the radial temperature gradient; and

(6) the power per unit area absorbed in the window P_A is given by

$$P_A(\rho/\rho_o) = P_I(\rho/\rho_o)(1-R)\left(1-e^{-\beta_A L_o}\right)\left(1-Re^{-\beta_A L_o}\right)^{-1} . \tag{33}$$

Here P_I is the incident power per unit area, R is the reflectivity of the window material, and β_A is the bulk absorption coefficient.

For $\beta_A L_o << 1$, Eq. (33) reduces to:

$$P_A(\rho/\rho_o) \cong P_I(\rho/\rho_o)\,\beta_A L_o . \tag{34}$$

3.2 Calculation of the Temperature Distribution

The equation of heat flow in the window is:

$$\frac{\partial T}{\partial t} = \frac{K}{c'}\nabla^2 T + \frac{Q}{c'} , \tag{35}$$

where K is the thermal conductivity, c' is the specific heat times the density, and Q, given by P_A/L_o, is the rate of heat generated within the window per unit volume. To give the reader some appreciation of the temperature distribution in cylindrical geometry, two model problems are presented from Carslaw and Jaeger (1959).

(1) Consider a disc, infinite along the ρ dimension and finite in z $(-L_o/2 \le z \le L_o/2)$. With zero initial temperature, zero surface temperatures, and Q constant for $t > 0$, the solution for $T(z,t)$ is given by Eq. (7), page 130 of Carslaw et al (1959). Its graph, depicted in our Figure 2, plots normalized temperature versus normalized distance with normalized time as parameters. The dominant term in the infinite series, namely, the first term, is proportional to $[1-\exp(-t/\tau_z)]$, where τ_z, the characteristic time for heat flow along the z axis, is given by $c' L_o^2/K\pi^2$. Consequently, for $t < \tau_z$, we see that to a fair approximation the temperature varies linearly with time.

(2) Consider the same disc as in (1) above. Besides a zero initial temperature and constant Q for $t > 0$, both faces at $z = \pm L_o/2$ transfer heat into a medium

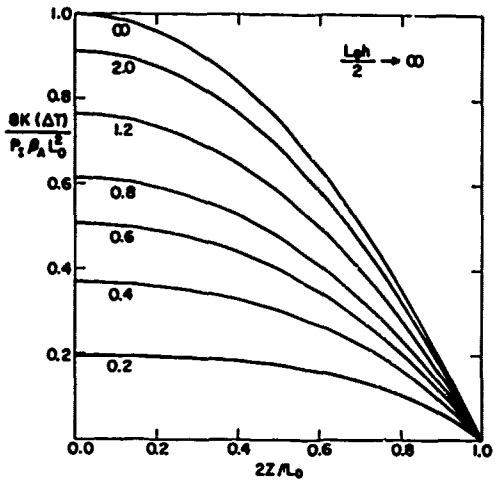

Figure 2. Normalized Temperature vs Normalized Axial Distance for the Case of a Disc, with Infinite Radius, at Zero Initial Temperature, Zero Surface Temperatures, and Constant Rate of Heat Generation. The numbers on the curves refer to normalized times $(8t/\pi^2\tau_z)$

at zero temperature. The solution for T(z, t, h) is given by Eq. (12), page 132 of Carslaw et al (1959). Its graphs, labelled in exactly the same fashion as Figure 2, are depicted in Figure 3 for three different dimensionless radiation parameters, $L_o h/2$; h is defined as the ratio of the surface heat transfer coefficient, or surface conductance, to the conductivity. Since the CGS dimensions of the surface transfer coefficient are $cal/cm^2\text{-}^oC\text{-}sec$, then h has dimensions of reciprocal length. Problem (1) could also be considered as a special case of problem (2), in which $L_o h/2$ is infinite.

Returning to our finite window, we choose to represent the power per unit area of the incident beam as any monotonically decreasing even function of ρ expandable in a convergent power series of the form:

$$P_I(\rho/\rho_o) = P(0) \sum_{l=0}^{\infty} (-1)^l P_{2l} (\rho/\rho_o)^{2l} . \tag{36}$$

Assuming time independence, and utilizing Eq. (34), Q can be expressed as:

$$Q(\rho/\rho_o) = \frac{P_A(\rho/\rho_c)}{L_o} \cong \beta_A P_I(\rho/\rho_o) . \tag{37}$$

If, in the heat equation, the Laplacian term becomes negligible compared with Q/c', then direct integration results in T being linearly dependent on t. That is,

$$T(\rho, t) \cong t\, Q/c' + T(0, 0) . \tag{38}$$

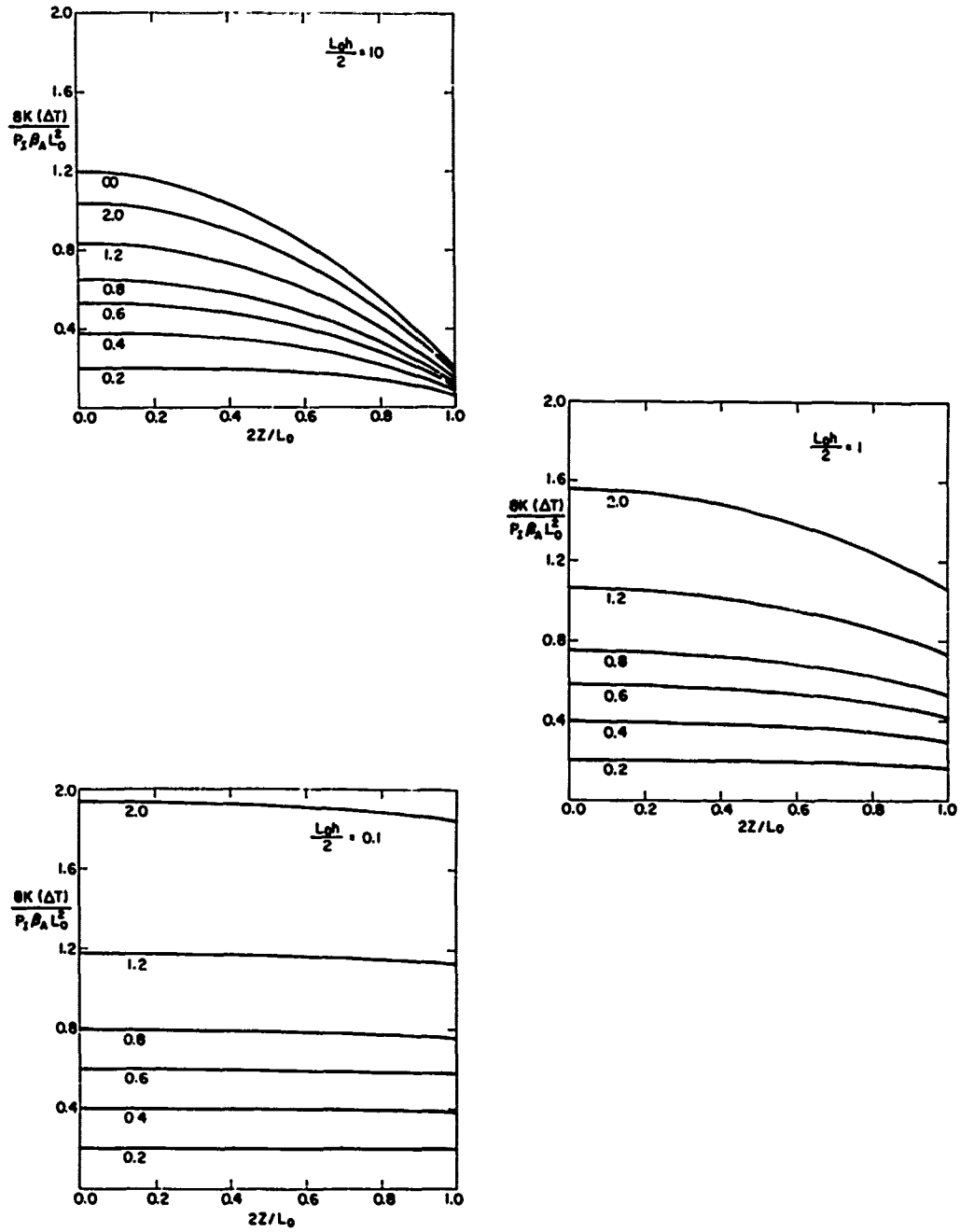

Figure 3. Normalized Temperature vs Normalized Axial Distance for the Case of a Disc with Infinite Radius, Zero Initial Temperature, Constant Rate of Heat Generation, and Both Faces Transferring Heat into a Zero Temperature Medium with Normalized Radiation Parameters (a) $L_o h/2 = 10$; (b) $L_o h/2 = 1.0$; and (c) $L_o h/2 = 0.1$. The numbers on the curves refer to normalized times $(8t/\pi^2 \tau_z)$

Initial uniform temperature has been assumed, and the z dependence has been neglected because it has negligible effect on the bending of a ray in the small angle-of-deviation approximation. Substituting Eqs. (37) and (36) into (38) produces:

$$T\left(\frac{\rho}{\rho_o}, t\right) = T(0,0) + \frac{\beta_A t P(0)}{c'} \sum_{\ell=0}^{\infty} (-1)^{\ell} P_{2\ell}\left(\frac{\rho}{\rho_o}\right)^{2\ell} . \tag{39}$$

We see that the form of T is the same as that assumed in Eqs. (2) and (3), where

$$g(t) = \frac{\beta_A t P(0)}{c'} \tag{40}$$

and

$$T_{2\ell} = (-1)^{\ell} P_{2\ell} . \tag{41}$$

P_o must also equal unity.

Let us now consider under what conditions the Laplacian term, $\left|\frac{K}{c'} \nabla^2 T(\rho, t)\right|$, would be much less than $|Q/c'|$. First, we assume that T has the form depicted in Eq. (39). Then, for cylindrical coordinates:

$$\frac{K}{c'} \nabla^2 T = \frac{K}{c'}\left[\frac{1}{\rho}\frac{\partial}{\partial \rho}\left(\rho \frac{\partial T}{\partial \rho}\right)\right] = \frac{tK\beta_A}{c'^2} P(0)\left(\frac{2}{\rho_o}\right)^2 \sum_{\ell=1}^{\infty} (-1)^{\ell} \ell^2 P_{2\ell}\left(\frac{\rho}{\rho_o}\right)^{2\ell-2} . \tag{42}$$

From Eqs. (37) and (36):

$$\frac{Q}{c'} = \frac{\beta_A}{c'} P(0) \sum_{\ell=0}^{\infty} (-1)^{\ell} P_{2\ell}\left(\frac{\rho}{\rho_o}\right)^{2\ell} . \tag{43}$$

For those cases in which both sums converge over the range of ρ and have values comparable in magnitude, it follows that $|(K/c')\nabla^2 T| << |Q/c'|$ when $t << c'\rho_o^2/4K$. We designate this quantity, $c'\rho_o^2/4K$, as τ_ρ, the characteristic time for heat flow along the ρ direction. It should be noted that, in general, any characteristic time for heat flow depends on cooling details.

Thus, we see that temperature will be approximately a linear function of time so long as $t < \tau_z$ and τ_ρ, respectively. Since the ratio τ_ρ/τ_z goes as $(\rho_o/L_o)^2$, which is much greater than unity, then τ_z is by far the smaller of the two quantities.

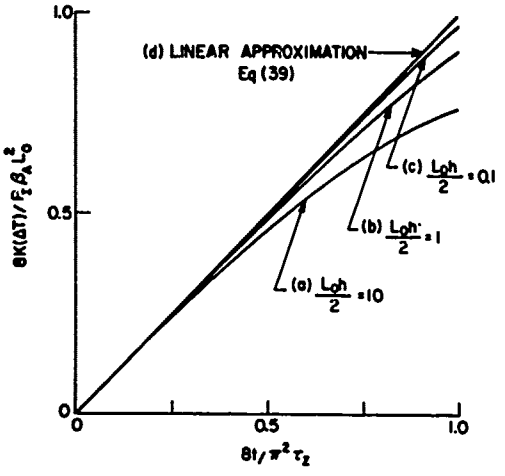

Figure 4. Normalized Temperature vs Normalized Time at the Center of the Infinite Disc Referred to in Figure 3. Curves (a) through (c) apply to Figures 3(a) through 3(c), respectively, while curve (d) is the approximate linear solution given by Eq. (39)

Consequently, we can conclude that the temperature behavior given by Eq. (39) is approximately valid for times less than τ_z.

Numerical values of τ_z for some materials under consideration will be quoted later.

We can get a quantitative estimate of just how valid this linear approximation is by reconsidering problem (2) mentioned above. Going back to Figures 3(a) through 3(c) we can obtain information about how normalized temperature varies with normalized time for the three different radiation parameters at, say, the center plane of the disc ($2z/L_o = 0$). We plot this data from these three figures in Figure 4 as curves (a) through (c), respectively. The line (d) represents the approximate linear solution given by Eq. (39). From Figure 4 we see that as $8t/\pi^2\tau_z$ varies from 0 to 1 the approximate linear solution is within about 3% of the exact solution for $L_o h/2 = 0.1$, within about 9% of the exact solution for $L_o h/2 = 1.0$, and within 24% for $L_o h/2 = 10$.

In the case of a finite disc in which ρ_o/L_o is still much larger than unity and for a given h, we can arrive at a more accurate g(t) function than the approximate linear solution. From the appropriate normalized temperature vs distance curves, as shown in Figure 3, for example, we could average each time-curve over the z coordinate, thereby eliminating the z-dependence of temperature. From this information, a normalized temperature vs time curve, similar to those shown on Figure 4, could be plotted and a g(t) function could be curve-fitted from it for use in Eq. (2).

3.3 Angular Deviations for Truncated Gaussian Beams in the Quartic Polynomial Approximation

If we choose the incident beam as having a truncated Gaussian power distribution given by

$$P_I(\rho/\rho_o) = P(0) \exp\left[-W\,(\rho/\rho_o)^2\right] \tag{44}$$

for $0 \leq \rho \leq \rho_o$, where W is a dimensionless constant, and make a quartic polynomial approximation to it, we obtain

$$P_I(\rho/\rho_o) \cong P(0)\left[1 - P_2\,(\rho/\rho_o)^2 + P_4\,(\rho/\rho_o)^4\right]. \tag{45}$$

Performing a least squares fit to determine P_2 and P_4, we find that for W = 1, $P_2 = 0.96$ and $P_4 = 0.33$, and that Eq. (45) fits Eq. (44) to within 1% everywhere; whereas for W = 2, $P_2 = 1.75$ and $P_4 = 0.93$, and Eq. (45) fits Eq. (44) to within 32% everywhere.

The formulas for θ_w^{ρ} and θ_w^{ϕ} in the quartic polynomial approximation (that is, $\ell = 1$ and 2 only) are given by Eq. (31) in conjunction with Eqs. (21), (40), and (41).

They are:

$$\theta_w^{\rho} = \left(\frac{2L_o t P(0)\beta_A}{\rho_o c'}\right)\left\{-P_2\left[\left(\frac{\partial n}{\partial T}\right)_{\sigma=o} + \frac{\alpha n^3}{8}\left((1-3\nu)p_{11}+(3-5\nu)p_{12}\right) + \alpha(1+\nu)(n-1)\right]\frac{\rho_i}{\rho_o}\right.$$

$$\left. + 2P_4\left[\left(\frac{\partial n}{\partial T}\right)_{\sigma=o} + \frac{\alpha n^3}{12}\left((1-5\nu)p_{11}+(5-7\nu)p_{12}\right) + \alpha(1+\nu)(n-1)\right]\left(\frac{\rho_i}{\rho_o}\right)^3\right\} \tag{46a}$$

and,

$$\theta_w^{\phi} = \left(\frac{2L_o t P(0)\beta_A}{\rho_o c'}\right)\left\{-P_2\left[\left(\frac{\partial n}{\partial T}\right)_{\sigma=o} + \frac{\alpha n^3}{8}\left((3-\nu)p_{11}+(1-7\nu)p_{12}\right) + \alpha(1+\nu)(n-1)\right]\frac{\rho_i}{\rho_o}\right.$$

$$\left. + 2P_4\left[\left(\frac{\partial n}{\partial T}\right)_{\sigma=o} + \frac{\alpha n^3}{12}\left((5-\nu)p_{11}+(1-11\nu)p_{12}\right) + \alpha(1+\nu)(n-1)\right]\left(\frac{\rho_i}{\rho_o}\right)^3\right\}. \tag{46b}$$

Utilizing the substitutions:

$$F_1^{\rho}(t) = \left(\frac{2L_o}{\rho_o}\right)P(0)P_2 t\left\{\left(\frac{\beta_A}{c'}\right)\left[\left(\frac{\partial n}{\partial T}\right)_{\sigma=o} + \frac{\alpha n^3}{8}\left((1-3\nu)p_{11}+(3-5\nu)p_{12}\right)\right.\right.$$

$$\left.\left. + \alpha(1+\nu)(n-1)\right]\right\}, \tag{47a}$$

$$F_2^{\rho} = \left(\frac{2P_4}{P_2}\right) \frac{\left(\frac{\partial n}{\partial T}\right)_{\sigma=o} + \frac{\alpha n^3}{12}\left((1-5\nu)p_{11} + (5-7\nu)p_{12}\right) + \alpha(1+\nu)(n-1)}{\left(\frac{\partial n}{\partial T}\right)_{\sigma=o} + \frac{\alpha n^3}{8}\left((1-3\nu)p_{11} + (3-5\nu)p_{12}\right) + \alpha(1+\nu)(n-1)}, \tag{47b}$$

for the ρ polarizations, and,

$$F_1^{\phi}(t) = \left(\frac{2L_o}{\rho_o}\right) P(0) P_2 t \left\{\left(\frac{\beta_A}{c'}\right)\left[\left(\frac{\partial n}{\partial T}\right)_{\sigma=o} + \frac{\alpha n^3}{8}\left((3-\nu)p_{11} + (1-7\nu)p_{12}\right) + \alpha(1+\nu)(n-1)\right]\right\}, \tag{48a}$$

$$F_2^{\phi} = \left(\frac{2P_4}{P_2}\right) \frac{\left[\left(\frac{\partial n}{\partial T}\right)_{\sigma=o} + \frac{\alpha n^3}{12}\left((5-\nu)p_{11} + (1-11\nu)p_{12}\right) + \alpha(1+\nu)(n-1)\right]}{\left[\left(\frac{\partial n}{\partial T}\right)_{\sigma=o} + \frac{\alpha n^3}{8}\left((3-\nu)p_{11} + (1-7\nu)p_{12}\right) + \alpha(1+\nu)(n-1)\right]}, \tag{48b}$$

for the ϕ polarizations, we can rewrite Eqs. (46a and b), for either polarization, as:

$$\theta_w^j = -F_1^j(t) \frac{\rho_i}{\rho_o}\left[1 + F_2^j\left(\frac{\rho_i}{\rho_o}\right)^2\right]. \tag{49}$$

We note that the F_1 and F_2 are functions of material parameters; F_1 may be of either sign, but, for all materials studied so far, F_2 is always positive and is typically less than unity. Under these circumstances, the qualitative behavior of θ_w^j will be governed by the sign of F_1^j. That is, depending on whether F_1^j is positive or negative, the window may act like a converging or diverging lens, respectively, having spherical aberration for each polarization. If more terms were kept in the approximation to the beam intensity, higher-order aberrations would appear.

4. THE DIFFRACTION-LIMITED TIME, t_d

Diffraction patterns in the scalar (Campbell et al, 1969) or vector (Bendow et al, 1972) Kirchhoff approximations can easily be calculated using modern computers. Such calculations do not, however, give the materials engineer much insight into how to design a better window, nor do they give the laser systems engineer a simple way of assessing the performance of known window materials. The object

of this work is to obtain approximate formulas of use to both types of investigators. To that end we give an approximate treatment of diffraction effects using a combination of geometrical optics and scalar Kirchhoff theory applied separately to the ρ and ϕ polarizations.

Initially, the spot size at focus in the far-field is determined only by diffraction. Aberrations produced by the window eventually dominate diffraction effects, however, and rapidly enlarge the spot size. We define the diffraction-limited time t_d as the time a laser-window system takes to pass from its diffraction-limited condition at $t = 0$ to its window-aberration-limited condition at $t = t_d$. In this section we compute t_d and show that it depends on window aberrations.

The diffraction half-angle θ_{diff} is a convenient approximate measure of the amount of spreading of a beam due to diffraction effects. We take it as that half-angle which contains 90% of the total diffracted power at the focused far-field spot. This can be obtained approximately by resorting to Figure 4 of Olaofe (1970). A horizontal line drawn from the ordinate 0.9 (which represents fractional power) intersects the $\eta = 1$ curve (which corresponds to our $W = 1$ case) at an abscissa value of approximately 3. This abscissa is the normalized radial distance, $(2\pi/\lambda)\rho_o\theta_{diff}$, where λ is the wavelength of the radiation. Equating the latter expression to 3, we obtain:

$$\theta_{diff} \cong \frac{3\lambda}{2\pi\rho_o}. \tag{50}$$

In the case of a beam prefocused to have a focal length R_o, the incident angle of deviation is given by $-\rho/R_o$. It can be added to θ_w^j [see Eq. (49)] to obtain the total angle of deviation:

$$\theta_{tot}^j = -\frac{\rho}{R_o} - F_1^j(t)\,\frac{\rho}{\rho_o}\left[1 - F_2^j\left(\frac{\rho}{\rho_o}\right)^2\right], \tag{51}$$

in which ρ has replaced ρ_i.

Because of the presence of the aberrating terms in Eq. (51), the rays incident at different ρ will not all come to a focus at the same range. Instead, the envelope of these rays will form a circle of least confusion. In Appendix D we calculate the time dependence of the radius and location of this circle of least confusion using geometrical optics, as depicted in Figure 5 for the quartic polynomial approximation.

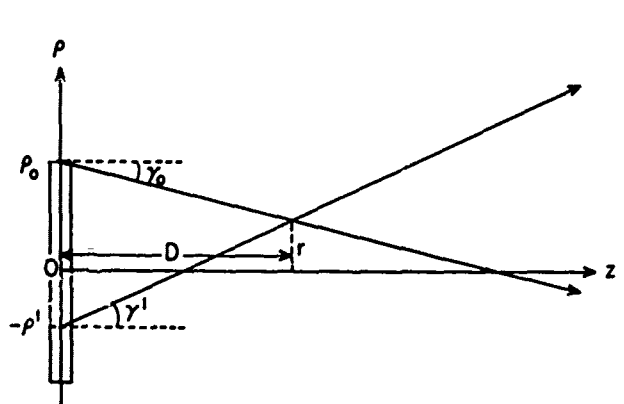

Figure 5. Two Rays Emanating from Two Different Radii Within the Window for the Case When γ Increases Monotonically with ρ. Their intersection (D, r) will give the distance and radius, respectively, of the circle of least confusion after r is maximized

The diffraction-limited time occurs when the radius of the circle of least confusion has grown so that it is equal to the radius of the diffraction circle. This latter radius, subtended by the angle θ_{diff} of Eq. (50), can be calculated in the small-angle approximation by multiplying θ_{diff} by its distance from the window. At the diffraction-limited time t_d this distance is also equal to $D_c^j(t_d)$, as given in Eq. (D-11) of Appendix D. Thus,

$$r_c^j(t_d) = \theta_{diff} D_c^j(t_d) . \tag{52}$$

Substituting Eqs. (50), (D-10), and (D-11) into Eq. (52) results in:

$$F_2^j F_1^j(t_d) = \frac{6\lambda}{\pi\rho_o} . \tag{53}$$

Depending on the polarization, either Eqs. (47a, b) or (48a, b) can be employed in the above equation. Solving for the time gives:

$$t_d^\rho = \left| \left(\frac{3\lambda}{2\pi L_o}\right)\left(\frac{1}{P(0)P_4}\right) \left\{ \frac{c'/\beta_A}{\left(\frac{\partial n}{\partial T}\right)_{\sigma=0} + \frac{\alpha n^3}{12}\left((1-5\nu)p_{11} + (5-7\nu)p_{12}\right) + \alpha(1+\nu)(n-1)} \right\} \right| \tag{54a}$$

for the ρ polarization, and,

$$t_d^{\phi} = \left| \left(\frac{3\lambda}{2\pi L_o}\right)\left(\frac{1}{P(0)P_4}\right) \left\{ \frac{c'/\beta_A}{\left(\frac{\partial n}{\partial T}\right)_{\sigma=0} + \frac{\alpha n^3}{12}\left((5-\nu)p_{11} + (1-11\nu)p_{12}\right) + \alpha(1+\nu)(n-1)} \right\} \right| \quad (54b)$$

for the ϕ polarization. Note that t_d^{ρ} and t_d^{ϕ} are independent of R_o, ρ_o, the quadratic term P_2, and the Gaussian focal lengths of the window [see Eqs. (32) and (21)]. The diffraction-limited time t_d serves as an excellent figure of merit for thermal lensing since it is independent of these quantities. Note also that the difference between t_d^{ρ} and t_d^{ϕ} for a given material serves as a measure of the importance of birefringence in determining the true diffraction patterns.

Figure 6 gives a graphical interpretation of t_d for the cases of D_c either decreasing or increasing with time.

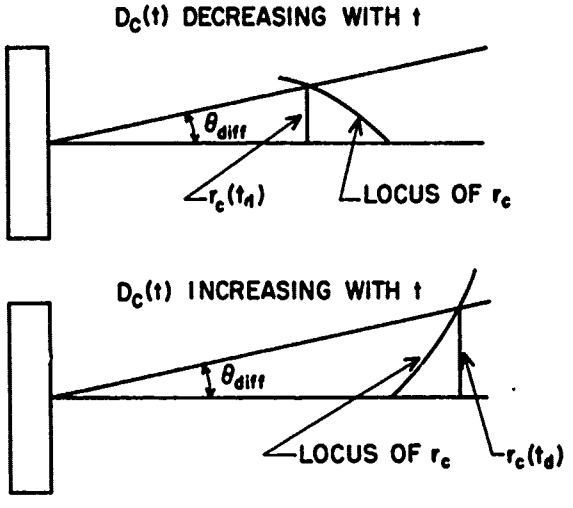

Figure 6. The Diffraction Half-Angle θ_{diff} and the Locus of the Radius of the Circle of Least Confusion $r_c(t)$ for Two Different Cases

There are two other quantities of interest which are calculated. The first is the temperature difference between the center of the window and its edge, denoted by $\Delta T(t)$. Referring back to Eq. (39) and employing only up to quartic terms in ρ/ρ_o, (that is, $\ell = 2$) the temperature difference becomes:

$$\Delta T(t) \equiv T(0,t) - T(1,t) = \left(\frac{\beta_A}{c'}\right) P(0)(P_2 - P_4)\, t. \quad (55)$$

The second quantity of interest is the amount of bulging in one face of the window, denoted by $\Delta L(t)$. Referring back to Eqs. (28), (40), and (41), and, proceeding as in the calculation of $\Delta T(t)$ above, we get:

$$\Delta L(t) \equiv L(0,t) - L(1,t) = \left(\frac{\beta_A}{c'}\right) P(0)\,(P_2 - P_4)\,\frac{L_o}{2}\,\alpha\,(1+\nu)\,t\,. \tag{56}$$

Thus, both $\Delta T(t)$ and $\Delta L(t)$ vary linearly in time in our approximation.

Values of t_d^{ρ}, t_d^{ϕ}, characteristic time τ_z, as well as those of ΔT and ΔL evaluated at the time t_d^{ρ}, have been computed for a number of candidate window materials for which reasonably complete data have been found. They are shown in Tables 1 and 2. In these computations we considered a Gaussian incident beam truncated at the e^{-1} power point and chose L_o = 3 cm with P(0) = 500 watts/cm^2. Note that for times approaching t_d in the I - VII and II - VII compounds the window experiences radial temperature differentials from center to edge in the tens of degrees, while the center of each face bulges out by factors several times that of the wavelength. The corresponding values for the other substances are very much smaller.*

The material dependent parameters used in these calculations were taken from the literature and are listed in Tables 3 and 4. These parameters should be considered as being representative only and are by no means definitive. The reason for this is that oftentimes the literature will report either many discrepant values, questionable values (for example, no listing of the wavelength or temperature at which the data was measured), or no values at all. Data on thermal conductivities seems to be especially erroneous. In such instances, one has to guess which values seem more reasonable compared with those of similar materials, or, to calculate an average value either from among all the listed data or from that which seems reasonable, or, to extrapolate from known data.

The value of Poisson's ratio hardly changes from substance to substance and was taken to be 0.3 throughout. The only exception to this was found to be TI No. 20 glass for which ν is 0.19.

For an e^{-2} truncated Gaussian beam the relative ordering of the materials by t_d^{ρ} and t_d^{ϕ} will not change but all of their values will decrease by a factor of 0.33/0.93 or by about 1/3.

We emphasize here that all formulas in this section are valid only for times less than or comparable to τ_z.

---

* We note here that the diffraction patterns for windows used under actual conditions will be very sensitive to small changes of shape of the window produced by nonthermal effects, that is, those produced by small vibrations or other mechanical disturbances.

Table 1. Calculations for Some Window Materials at $\lambda = 10.6\ \mu$

Material	t_d^ρ(sec)	t_d^ϕ (sec)	τ_z (sec)	$\Delta T(t_d^\rho)$ in °C	$\Delta L(t_d^\rho)$ in μ	$(\partial n/\partial T)_{\sigma=0}$ $\times 10^5$	(Elasto-Optic)$^\rho$ $\times 10^5$	(Elasto-Optic)$^\phi$ $\times 10^5$	$\alpha(1+\nu)(n-1)$ $\times 10^5$
I-VII: KBr	(4420)*	(10,000)*	23	(61)	(52)	-4.00	0.49	0.80	2.96
KCl	(190)*	(3400)*	19	(124)	(87)	-2.75	0.33	0.58	2.15
Na Cl	(120)*	(160)*	26	(30)	(26)	-2.20	0.52	0.25	2.80
KI	(100)*	(150)*	36	(35)	(29)	-5.00	0.59	0.91	3.43
CsI	16.4	16.4	73	7.8	7.7	-9.10	---	---	4.80
CsBr	12.4	12.4	111	15	14	-6.30	---	---	4.12
KRS-5	2.9	2.9	245	3.3	3.8	-23.5	3.09	3.09	10.3
II-VI: CdTe	7.3	7.0	31	2.8	0.2	11.0	-0.05	0.47	0.94
ZnSe	1.1	1.0	2.8	5.3	0.7	4.80	-0.06	0.57	1.27
III-V: GaAs	0.7	0.7	3.1	1.6	0.2	18.7	-0.58	-0.82	1.79
InSb	0.2	0.2	5.5	0.6	0.05	55.2	1.21	1.21	1.88
IV: Ge	0.3	0.3	2.5	1.0	0.1	27.0	1.75	2.33	2.34
Glasses:									
TI #1173	0.5	0.5	391	2.6	0.8	7.9	1.06	1.06	3.12
TI # 20	0.4	0.4	465	2.8	0.7	7.9	1.34	1.34	2.36
Polycrystals:									
Irtran-4 (ZnSe)	0.4	0.3	19	5.2	0.8	4.80	-0.07	0.66	1.46
Irtran-6 (CdTe)	0.08	0.08	27	---	---	11.0	-0.07	0.64	1.24

* Values much larger than τ_z have no meaning as a diffraction-limited time but are included only to give the reader a basis for the relative ordering of these materials with regard to aberrations effects.

Table 2. Calculations for Some Window Materials for $3\mu \leq \lambda \leq 5\mu$

Material	$\lambda(\mu)$	t_d^{ρ}(sec)	t_d^{ϕ}(sec)	τ_z(sec)	$\Delta T(t_d^{\rho})$ in °C	$\Delta L(t_d^{\rho})$ in μ	$(\partial n/\partial T)_{\sigma=0}$ $\times 10^5$	(Elasto-Optic)$^{\rho}$ $\times 10^5$	(Elasto-Optic)$^{\phi}$ $\times 10^5$	$\alpha(1+\nu)(n-1)$ $\times 10^5$
I-VII: LiF	4	(130)*	(210)*	29	(54)	(37)	-1.60	0.25	-0.14	1.59
II-VII: SrF_2	4	(160)*	(50)*	23	(103)	(39)	-1.19	-0.05	0.46	1.12
BaF_2	4	(100)*	(30)*	15	(82)	(32)	-1.70	0.38	-0.01	1.17
CaF_2	4	(36)*	(130)*	25	(22)	(8.6)	-0.77	0.28	-0.14	1.07
II-VI: ZnS	4	1.2	1.2	9.1	2.0	0.2	5.20	-0.05	0.27	1.02
MgO	5	1.1	1.4	7.4	5.7	1.2	1.90	-0.03	-0.52	0.90
III-V: GaP	5	1.5	1.5	2.9	1.3	0.2	10.0	-0.21	-0.68	1.51
IV: Si	4	(2.3)*	(2.2)*	1.3	(0.9)	(0.04)	13.4	-0.01	0.29	0.76
Ge	4	0.7	0.7	2.5	0.4	0.05	27.0	1.78	2.37	2.36
Other Crystals: YAG	3	5.3	5.5	23	6.1	0.9	0.73	0.02	-0.06	0.81
Glasses: $Ca_3Al_2O_6$ (BS39B)	3	2.1	2.1	557	5.2	1.0	0.83	0.17	0.17	0.80
$Ca_3Al_2O_6$ (BS37A)	3	0.9	0.9	449	6.1	0.9	0.83	0.13	0.13	0.60
As_2S_3	4	0.3	0.3	783	1.9	0.9	0.19	1.96	2.08	4.31

* Values much larger than τ_z have no meaning as a diffraction-limited time but are included only to give the reader a basis for the relative ordering of these materials with regard to aberrations effects.

Table 3. Values of Parameters Used in Calculations at $\lambda = 10.6\mu$

Material	$C'\left(\frac{J}{cm^3-{}^oK}\right)$	$\alpha({}^oK)^{-1}\times 10^5$	$K\left(\frac{W}{cm-{}^oK}\right)\times 10^2$	n	$\beta_A(cm)^{-1}\times 10^3$	$p_{11}\times 10$	$p_{12}\times 10$
I-VII: KBr	1.20	4.30	4.80	1.53	* 0.05	2.15	1.68
KCl	1.35	3.60	6.53	1.46	2.7	2.09	1.56
NaCl	1.85	4.40	6.49	1.49	1.34	1.26	1.68
KI	0.983	4.26	2.50	1.62	* 1.0	2.13	1.72
CsI	0.906	5.00	1.13	1.74	1.3	--	--
CsBr	1.17	4.79	0.96	1.66	4.4	--	--
KRS-5	* 1.45	5.80	0.54	2.37	5.0	* 2.0	* 2.0
II-VI: CdTe	1.37	0.45	4.10	2.60	1.6	* 1.5	* 0.0
ZnSe	0.379	0.70	12.14	2.40	* 6.0	* 1.5	* 0.0
III-V: GaAs	1.55	0.60	46.00	3.30	12.0	-1.65	-1.40
InSb	1.20	0.49	20.00	3.95	8.6	* 2.0	* 2.0
IV: Ge	1.65	0.60	60.00	4.00	19.0	2.7	2.35
Glasses:							
TI 1173	1.29	1.50	0.30	2.60	20.0	* 2.0	* 2.0
TI 20**	1.33	1.33	0.26	2.49	*30.0	2.1	2.1
Polycrystals:							
Irtran-4 (ZnSe)	2.65	0.80	12.98	.41	122	* 1.5	* 0.0
Irtran-6 (CdTe)	1.22	0.57	4.10	2.67	120	* 1.5	* 0.0

* Estimated values

** $\nu = 0.19$ for this material

Table 4. Values of Parameters Used in Calculations for $3\mu \leq \lambda \leq 5\mu$

Material	$\lambda(\mu)$	$C'\left(\frac{J}{cm^3-{}^oK}\right)$	$\alpha({}^oK)^{-1} \times 10^5$	$K\left(\frac{W}{cm-{}^oK}\right)\times 10^2$	n	$\beta_A(cm)^{-1} \times 10^3$	$p_{11}\times 10$	$p_{12}\times 10$
I-VII: LiF	4	4.12	3.50	0.13	1.35	* 5	0.19	1.22
II-VII: SrF_2	4	2.55	1.95	0.10	1.44	* 5	* 2.0	* 0.0
BaF_2	4	1.95	2.00	0.117	1.45	* 5	1.31	2.77
CaF_2	4	2.71	2.00	0.10	1.41	* 5	0.41	2.15
II-VI: ZnS	4	1.99	0.63	0.20	2.25	*10	0.91	-0.10
MgO	5	3.23	1.10	0.40	1.63	50	-3.20	-0.80
III-V: GaP	5	3.49	0.58	1.10	3.00	*10	-1.51	-0.82
IV: Si	4	1.70	0.24	1.20	3.43	* 2	0.81	0.10
Ge	4	1.65	0.60	0.60	4.02	3	2.70	2.35
Other Crystals:								
YAG	3	2.85	0.79	0.111	1.79	*10	-0.29	0.09
Glasses:								
$Ca_3Al_2O_6$ (BS39B)	3	2.69	0.97	0.004	1.64	20	* 2.0	* 2.0
$Ca_3Al_2O_6$ (BS37A)	3	2.46	0.74	0.005	1.63	50	* 2.0	* 2.0
As_2S_3	4	1.46	2.35	0.002	2.41	29	3.08	2.99

* Estimated values

5. DISCUSSION

5.1 Diffraction-Limited Time

Equations (54 a, b) show that the material-dependent portion of t_d is directly proportional to the ratio c'/β_A and inversely proportional to the sum of three terms. The first two terms of this sum are contributions to the spherical aberration coming from the gradient in the refractive index. We will refer to the second quantity as the "elasto-optical" term. The third term arises from the window's bulging, and, under the prevailing circumstances, always makes a positive contribution. With regard to the substances studied, the numerical values corresponding to each of these terms, including the elasto-optic for both polarizations, are listed in the last four columns of Tables 1 and 2.

For the I - VII and II - VII compounds, $(\partial n/\partial T)_{\sigma=0}$ is negative and of comparable magnitude to $\alpha(1+\nu)(n-1)$. Therefore, these two terms almost cancel. This allows the elasto-optic terms to play a very significant role even though they are typically an order of magnitude smaller.

For covalent crystals $(\partial n/\partial T)_{\sigma=0}$ is observed to be positive and larger than $\alpha(1+\nu)(n-1)$, which, in turn, is larger than either elasto-optic quantity. Thus, the elasto-optic terms will have a small effect.

In glasses, $(\partial n/\partial T)_{\sigma=0}$ and $\alpha(1+\nu)(n-1)$ are both positive, comparable in magnitude, and only slightly greater than the elasto-optic quantities. The only glaring exception is As_2S_3 glass, for which the elasto-optic terms at 4μ are comparable to $\alpha(1+\nu)(n-1)$ and both elasto-optic terms are at least an order of magnitude greater than $(\partial n/\partial T)_{\sigma=0}$.

One should recall that the values of t_d given in Tables 1 and 2 are accurate only if the assumptions listed in Section 3 are valid. Actual materials may not perform as well.

5.2 Relative Merits of Candidate Window Materials

One must also remember that the diffraction-limited time is but one factor in the selection of a window material for a particular application. In the following discussion of the relative performance of materials listed in Tables 1 and 2, we will include some of these other factors.

For 10.6-micron operation the alkali halide crystals listed in Table 1 are much better in their ability to hold a diffraction-limited focus than any other class of materials studied. Their single-crystalline mechanical properties are, however, generally poor. They are hygroscopic and they cannot easily be coated for protective or antireflective purposes. The II-VI and III-V crystals have fair mechanical properties but are, in general, only marginal in terms of beam

distortion. In addition, one expects some difficulty in growing large-size optical-quality crystals of these materials. From a thermal lensing point of view CdTe appears to be quite a bit better than ZnSe or the III-V's examined in Table 1. Perhaps, as better samples of the other materials are prepared, thereby producing lower values of β_A, for example, these samples may become more competitive with CdTe. Germanium has a rather low diffraction-limited time but its other properties are good except for its large index of refraction. With an index of 4, Ge would probably require antireflective coatings. The TI glasses have good mechanical properties and can be cast in large sizes but have rather low values for t_d. In addition, they have characteristic thermal times (τ_z and τ_ρ) which are quite large and would probably require rapid face cooling even for pulsed laser operation. The polycrystalline materials shown in Table 1 have values of t_d that are too low but have good mechanical and thermal properties. In general, polycrystalline materials would show more promise if techniques could be found to reduce their bulk absorption coefficients closer to intrinsic, single-crystalline values.

The situation for 3- to 5-micron laser operation is somewhat better. The I-VII and II-VII compounds shown in Table 2 all appear to be good candidate windows: they hold a diffraction limited focus for a long time; they have good mechanical and thermal properties, are not hygroscopic, and, from all indications, large optical quality crystals can be grown. The remaining materials shown in Table 2 are, at best, only marginal from a thermal lensing point of view. As more data becomes available, other materials may also be found which are good candidates for 3- to 5-micron operation.

6. SOME APPROACHES TO SOLVING THE THERMAL LENSING PROBLEM

6.1 Material-Type Solutions

6.1.1 MINIMIZE β_A

One of the most obvious ways to minimize aberration effects is to find a material with a very small β_A and with negligible beam energy losses by other mechanisms. This may involve synthesizing a very pure solid or designing a completely new material..

6.1.2 MUTUAL CANCELLATION OF ABERRATING TERMS

From an inspection of Eq. (54) it is clear that t_d^j is large if the denominator in the material dependent term is small. If a substance could be synthesized or designed such that

$$\left(\frac{\partial n}{\partial T}\right)_{\sigma=0} + [\text{elasto-optic term}]^{j} + \alpha(1+\nu)(n-1) = 0 , \qquad (57)$$

then there would be no aberration for that polarization in the quartic approximation to the truncated Gaussian beam. In fact, this effect is quite prominent in the I - VII and II - VII compounds shown in Tables 1 and 2. This shows that it may be possible to find or design an ionic material where Eq. (57) is fulfilled. Satisfying Eq. (57) would not eliminate all aberration, since there would still be a small amount resulting from the terms that we neglected in Eq. (31).

6.1.3 COMPOSITE WINDOW

It is possible, in principle, to find two different materials, one with a positive θ_w and the other with a negative θ_w of the same magnitude, such that when they act in series as a composite window the aberrations nearly cancel out. If two such materials could be found, a diffraction-limited focus could be maintained for a long time.

6.2 Engineering-Type Solutions

6.2.1 COOLING

One method of minimizing the thermally-induced aberrations is to cool the window in such a way as to minimize the temperature gradient in the ρ direction. We can imagine several schemes of forced face-cooling below ambient temperature which may accomplish this, and these, as well as other cooling configurations, should be thoroughly studied. If one face-cools too rapidly, however, large temperature gradients in the z direction will be set up which could either permanently strain the window or crack it.

6.2.2 MOVING WINDOW OR MOVING BEAM

Another engineering possibility suggested by M. Sparks is to minimize thermal effects by moving a large window with respect to a smaller laser beam. This would allow the beam to travel through fresher material than if the entire system had been fixed. After the exposed portion of the window rotated away from the beam, it could be cooled.

6.2.3 OPTICAL COMPENSATION

A very appealing solution would be to compensate fully for window aberrations by designing a continually changing fore-optical system. This system would have to change shape in such a manner that it caused the incident angle at the window to be given by:

$$\theta^j_{comp} = -\frac{\rho}{R_o} + F^j_1(t)\frac{\rho}{\rho_o}\left[1 - F^j_2\left(\frac{\rho}{\rho_o}\right)^2\right] . \quad (58)$$

When θ^j_{comp} was added to θ^j_w [given by Eq. (49)], the resulting total angle of deviation would be:

$$\theta^j_{tot} = -\frac{\rho}{R_o} . \quad (59)$$

This means that no spherical aberration would occur and that the beam would remain diffraction-limited for a long time.

7. PROGRAM RESEARCH AND DEVELOPMENT NEEDS

In this section, we list some laser window program needs in the area of materials research and development.* We divide them into three areas: immediate R and D objectives as well as longer-term experimental and theoretical studies.**

7.1 Some Specific Immediate R and D Objectives

7.1.1 TO OBTAIN DATA

More and better data on key material parameters are needed at both 10.6μ and 3 to 5μ so that prospective window candidates may be properly evaluated. These important parameters are:

(a) bulk absorption coefficient β_A ;
(b) specific heat c' ;
(c) linear expansion coefficient α :
(d) index of refraction n :
(e) temperature coefficient of index of refraction $\left(\frac{\partial n}{\partial T}\right)_{\sigma=o}$
(f) Poisson's ratio ν ;
(g) Pockel's elasto-optic constants p_{ij}; and,
(h) thermal conductivity K .

---

* A brief discussion of some of these needs was presented by Dr. J. R. Jasperse at the ARPA-sponsored meeting on laser window materials at Wood's Hole, Mass. in July, 1971.

** This list should not be considered as exhaustive or as representative of the current laser window program at AFCRL. It gives the authors' thoughts on some of the more important program needs as of July 1971.

For many materials of interest, data are just not available; whereas in other cases they are not reliable.

7.1.2 TO IMPROVE AND DEVELOP SOME SPECIFIC CANDIDATE MATERIALS

(a) Alkali Halides

Here, work in the immediate future should be centered around the two objectives of improving the mechanical properties of the I - VII's and reducing their propensity to pick up water.

(b) II - VI's and III - V's

Two aspects of research and development should be emphasized here: (1) growth of crystals of increased purity and improved optical quality, so as to produce materials that achieve a β_A approaching its intrinsic value; and, (2) development of large-size growth techniques since difficulties are anticipated in growing large crystals of these materials.

(c) Glasses

Research and development on glasses should be geared toward solving the problem of designing a glass with a small β_A and with an increased thermal conductivity. Large-size window fabrication should not be a major problem for the glasses, since modest-sized castings are currently available with present technology.

(d) Polycrystalline Materials

The important objective here is to make polycrystalline aggregates with β_A close to intrinsic values. This would provide window materials which could be formed in large sizes and yet have small values for β_A.

7.2 Some Specific Experimental Studies Needed

(1) The optical properties of polycrystalline materials as a function of grain size. These studies should be carried out for both a cubic and a noncubic material chosen such that grain sizes can be varied over a wide range compared with the wavelength of the light.

(2) The influence of impurities and defect structure on the optical properties of candidate crystals.

(3) The surface and bulk scattering properties of real candidate materials.

(4) The surface and bulk absorption properties of real candidate materials.

(5) Determination of the intrinsic dielectric breakdown limit in real candidate materials as power densities are increased over those currently anticipated.

(6) The development of coating technology for all candidate materials, especially for the alkali halides where difficulties are known to exist.

(7) Energy-loss mechanisms studies.

7.3 Some Specific Theoretical Studies Needed

(1) A fundamental theory for n and β_A in dielectric crystals which is accurate in the vicinity of 10.6 microns.

(2) A fundamental study of why $\left(\frac{\partial n}{\partial T}\right)_{\sigma=0}$ is negative for ionic crystals and positive for covalent crystals.

(3) A fundamental model for the elasto-optic coefficients accurate in the vicinity of 10.6 microns.

(4) A study of the effect of coherent light on the absorption of power in a disc-shaped laser window.

(5) A study of the effect of surface absorption on thermal lensing and on localized heating.

(6) A study of the effect of surface and bulk scattering on the temperature distribution in the laser window.

(7) Studies on how to design a new material with a maximum diffraction-limited time and with other desirable physical properties.

(8) Calculations of ω versus k in prospective window materials to include some ternary compounds.

Acknowledgments

We express our appreciation for meaningful discussions with Dr. M. Sparks, Dr. N.G. Parke III, H. Winsor, Capt, USAF, and Dr. C.M. Stickley.

References

Bendow, B., Jasperse, J.R., and Gianino, P.D. (1972) Kirchhoff diffraction . theory of thermal lensing in solids, Optical Communications.

Boley, B. and Weiner, J.H. (1960) Theory of Thermal Stresses, John Wiley and Sons, Inc., New York.

Born, M. and Wolf, E. (1964) Principles of Optics, second (revised) edition, Macmillan Co., New York, p. 123, 124.

For example, see Campbell, J.P., and DeShazer, L.G. (1969) J. Opt. Soc. Amer. 59:1427.

Carslaw, H.S., and Jaeger, J.C. (1959) Conduction of Heat in Solids, second edition, Oxford Press, London.

For a review of recent developments see Emmett, J.L. (1971) Physics Today 24, No. 3:24.

Foster, J.D., and Osterink, L.M. (1970) J. Appl. Phys. 41:3656 and Koechner, W. (1970) Appl. Opt. 9:2548.

Gordon, J.P., Leite, R.C.C., Moore, R.S., Porto, S.P.S. and Whinnery, J.R., (1965) J. Appl. Phys. 36:3.

Horrigan, F., Klein, C., Rudko, R. and Wilson, D. (1969) Microwaves 8:68.

Jasperse, J.R. and Gianino, P.D. (1972) J. Appl. Phys. 43:1686.

Krishnan, R.S. (1958) Progress in Crystal Physics, Vol. I (S. Viswanathan, Madras, India).

Olaofe, G.O. (1970) J. Opt. Soc. Amer. 60:1654.

Quelle, F.W., Jr. (1966) Appl. Opt. 5:633.

Sparks, M. (1971) Optical Distortion by Heated Windows in High-Power Laser Systems, The Rand Corp., R-545-PR, (Apr. 1971) (unpublished), and J. Appl. Phys. 42:5029.

Tien, P.K., Gordon, J.P., and Whinnery, J.R. (1965) Proc. IEEE 53:129.

Whinnery, J.R. (1965) J. Appl. Phys. 36:3.

Whinnery, J.R., Miller, D.T., and Dabby, F. (1967) IEEE, J. Quantum Electron, 3:382.

Appendix A

Derivation of the Polarization-Dependent Refractive Indices as Power Series in ρ/ρ_o

In order to evaluate the two integrals in Eqs. (19a and b), we must first determine ΔT. Substituting Eqs. (2) and (3) into (16) and replacing ρ/ρ_o by q, we get:

$$\Delta T(q, t) = g(t) \sum_{\ell=o}^{\infty} T_{2\ell}\, q^{2\ell} \,. \tag{A-1}$$

Then,

$$\int_o^q dx\, x\, \Delta T(x, t) = g(t) \sum_{\ell=o}^{\infty} T_{2\ell} \int_o^q dx\, x^{2\ell+1} = g(t) \sum_{\ell=o}^{\infty} \frac{T_{2\ell}}{2\ell+2}\, q^{2\ell+2} \tag{A-2}$$

and

$$\int_o^1 dx\, x\, \Delta T(x, t) = g(t) \sum_{\ell=o}^{\infty} \frac{T_{2\ell}}{2\ell+2} \,. \tag{A-3}$$

When these integrals are inserted into Eqs. (19), there results:

$$\sigma_{\rho\rho} = \alpha\, Y\, g(t) \sum_{\ell=o}^{\infty} \frac{T_{2\ell}}{2\ell+2} \left\{1 - q^{2\ell}\right\} , \tag{A-4}$$

and

$$\sigma_{\phi\phi} = \alpha\, Y\, g(t) \sum_{\ell=0}^{\infty} \frac{T_{2\ell}}{2\ell+2} \left\{ 1 - (2\ell+1)\, q^{2\ell} \right\} . \tag{A-5}$$

From Eq. (12):

$$n_\rho - n = \left(\frac{\partial n}{\partial T}\right)_{\sigma=0} g(t) \sum_{\ell=0}^{\infty} T_{2\ell}\, q^{2\ell} - \frac{n^3}{2Y} \left[C_0 \sigma_{\rho\rho} + C_1 \sigma_{\phi\phi} \right] . \tag{A-6}$$

Upon substituting Eqs. (14), (15), (A-4), and (A-5) into the above and solving for n_ρ :

$$n_\rho = n + \left(\frac{\partial n}{\partial T}\right)_{\sigma=0} g(t) \sum_{\ell=0}^{\infty} T_{2\ell}\, q^{2\ell} - \frac{n^3}{2} \alpha\, g(t) \sum_{\ell=0}^{\infty} \frac{T_{2\ell}}{2\ell+2}$$

$$\left\{ \left[p_{11} - 2\nu p_{12} \right] \left[1 - q^{2\ell} \right] + \left[(1-\nu) p_{12} - \nu p_{11} \right] \left[1 - (2\ell+1) q^{2\ell} \right] \right\} . \tag{A-7}$$

This can be rearranged to:

$$n_\rho = n + g(t) \sum_{\ell=0}^{\infty} T_{2\ell} \left\{ \left(\frac{\partial n}{\partial T}\right)_{\sigma=0} q^{2\ell} - \frac{\alpha n^3}{2(2\ell+2)} \left[(1-\nu) p_{11} \right. \right.$$

$$\left. \left. + (1-3\nu) p_{12} - q^{2\ell} \left\{ (1-(2\ell+1)\nu)\, p_{11} + (2\ell+1-(2\ell+3)\nu)\, p_{12} \right\} \right] \right\} . \tag{A-8}$$

We now partition the summation into two terms: one being the summand evaluated at $\ell = o$, the other being the sum from one to infinity. When this is done, one can easily see that there will be some terms that do not contain q. These are collected under the symbol $n_\rho(0, t)$, leaving:

$$n_\rho = n_\rho(0, t) + g(t) \sum_{\ell=1}^{\infty} T_{2\ell}\, q^{2\ell} \left\{ \left(\frac{\partial n}{\partial T}\right)_{\sigma=0} + \frac{\alpha n^3}{2(2\ell+2)} \right.$$

$$\left. \left[(1-(2\ell+1)\nu) p_{11} + (2\ell+1 - (2\ell+3)\nu) p_{12} \right] \right\} . \tag{A-9}$$

This can be rewritten as:

$$n_\rho = n_\rho(0,t) + g(t) \sum_{\ell=1}^{\infty} n_{2\ell}^{\rho} \, q^{2\ell} \, , \tag{A-10}$$

which is Eq. (20a), and where

$$n_{2\ell}^{\rho} = T_{2\ell} \left\{ \left(\frac{\partial n}{\partial T} \right)_{\sigma=0} + \frac{\alpha n^3}{2(2\ell+2)} \left[(1-(2\ell+1)\nu)p_{11} + (2\ell+1-(2\ell+3)\nu)p_{12} \right] \right\} , \tag{A-11}$$

which is Eq. (21a).

The same line of reasoning pertains to $n_\phi(q,t)$. In its counterpart to Eq. (A-6), the n_ρ is replaced by n_ϕ, and the C_0 and C_1 are interchanged. Thus, the counterpart to what is inside the braced term in Eq. (A-7) becomes:

$$\left\{ \left[(1-\nu)p_{12} - \nu p_{11} \right] \left[1 - q^{2\ell} \right] + \left[p_{11} - 2\nu p_{12} \right] \left[1 - (2\ell+1) q^{2\ell} \right] \right\},$$

which can be rearranged to:

$$\left[(1-\nu)p_{11} + (1-3\nu)p_{12} - q^{2\ell} \left\{ (2\ell+1-\nu)p_{11} + (1-(4\ell+3)\nu)p_{12} \right\} \right].$$

Again, partitioning the sum into two terms and collecting all terms not containing q under the symbol $n_\phi(0,t)$, this leaves:

$$n_\phi = n_\phi(0,t) + g(t) \sum_{\ell=1}^{\infty} n_{2\ell}^{\phi} \, q^{2\ell} \, , \tag{A-12}$$

which is Eq. (20b), where

$$n_{2\ell}^{\phi} = T_{2\ell} \left\{ \left(\frac{\partial n}{\partial T} \right)_{\sigma=0} + \frac{\alpha n^3}{2(2\ell+2)} \left[(2\ell+1-\nu)p_{11} + (1-(4\ell+3)\nu)p_{12} \right] \right\} , \tag{A-13}$$

which is Eq. (21b).

Appendix B

Approximate Solution to Ray Trace Equation

According to the ray-trace formulas, the radius of curvature R_c at any point on the ray trajectory is (Born et al, 1964):

$$\frac{1}{R_c} = \hat{\nu} \cdot \vec{\nabla} (\ell n\, n) = \left|\vec{\nabla}(\ell n\, n)\right| \cos\theta \quad , \tag{B-1}$$

where $\hat{\nu}$ is the unit normal along R_c and n represents either n^{ρ} or n^{ϕ} (See Figure 1). From elementary calculus the radius of curvature of a simple plane curve is

$$\frac{1}{R_c} = \frac{d^2\rho/dz^2}{\left[1 + \left(\frac{d\rho}{dz}\right)^2\right]^{3/2}} .$$

Consider an index of refraction which depends only on ρ, and which is either monotonically increasing or monotonically decreasing, so that the algebraic sign of R_c does not change. If we equate the right-hand side of the two equations above, and replace $\cos\theta$ by $[1 + \tan^2\theta]^{-1/2}$, where $\tan\theta = d\rho/dz$, then we obtain the following nonlinear, second-order differential equation for the ray trajectory:

$$\frac{d^2\rho}{dz^2} - \left[1 + \left(\frac{d\rho}{dz}\right)^2\right]\left(\frac{1}{n}\right)\frac{dn}{d\rho} = 0 . \qquad \text{(B-2)}$$

For small angles of deviation, $\left(\frac{d\rho}{dz}\right)^2$ is negligible compared to unity. *

Since we are assuming refractive indices of the form shown in Eqs. (20a) or (20b), the $dn/d\rho$ are calculable as power series and the n in the denominator of Eq. (B-2) can be approximated by $n(0,t)$. The nonlinear equation becomes:

$$\frac{d^2\rho}{dz^2} - \left(\frac{2\,g(t)}{n(0,t)\rho_o}\right)\sum_{\ell=1}^{\infty} n_{2\ell}\,\ell\,(\rho/\rho_o)^{2\ell-1} = 0 . \qquad \text{(B-3)}$$

Looking for a solution of the form

$$\rho(z) = \rho_i\,[1 + y(z)] ,$$

where $|y| \ll 1$, we obtain

$$\frac{d^2y}{dz^2} - \left(\frac{2\,g(t)}{n(0,t)\rho_o\rho_i}\right)\sum_{\ell=1}^{\infty} n_{2\ell}\,\ell\left(\frac{\rho_i}{\rho_o}\right)^{2\ell-1}(1+y)^{2\ell-1} = 0 . \qquad \text{(B-4)}$$

Expanding $(1+y)^{2\ell-1}$ up to first-order in y, the differential equation can be written as:

$$\frac{d^2y}{dz^2} - 2\,K(t) - 2\,K'(t)\,y = 0 , \qquad \text{(B-5)}$$

where

$$K(t) = \frac{g(t)}{n(0,t)\rho_o\rho_i}\sum_{\ell=1}^{\infty} n_{2\ell}\,\ell\left(\frac{\rho_i}{\rho_o}\right)^{2\ell-1} , \qquad \text{(B-6)}$$

and

$$K'(t) = \frac{g(t)}{n(0,t)\rho_o\rho_i}\sum_{\ell=1}^{\infty} n_{2\ell}\,\ell\,(2\ell-1)(\rho_i/\rho_o)^{2\ell-1} . \qquad \text{(B-7)}$$

Employing the boundary conditions that $y = dy/dz = 0$ at $z = 0$, we can get 2 possible solutions for y, depending on the sign of K'. For $K' > 0$,

---

*This is equivalent to the paraxial-ray approximation.

$$y = \frac{K}{K'}\left\{\cosh\sqrt{2K'}\ z - 1\right\}.$$

Or, expanding up to order K^3z^6, remembering that K and K' have the same order of magnitude:

$$y \cong Kz^2 + \frac{KK'}{6} z^4 + O\left\{K^3 z^6\right\};$$

whereas, for $K' < 0$,

$$y = -\frac{K}{|K'|}\left\{\cos\sqrt{2\,|K'|}\ z - 1\right\}.$$

Again, expanding,

$$y \cong Kz^2 - \frac{K|K'|}{6} z^4 + O\left\{|K|^3 z^6\right\}.$$

Thus, for either case, the solution can be expressed as:

$$\rho(z) = \rho_i\left[1 + Kz^2 + \frac{|K|\ |K'|}{6} z^4 + O\left\{|K|^3 z^6\right\}\right], \qquad \text{(B-8)}$$

where K can be either positive or negative.

Appendix C

Derivation of Equation (29)

Figure C1 depicts a ray, incident at $\rho=\rho_i$, being refracted at each surface of the bulging window. All angles are exaggerated for clarity. The i's represent incident angles at each surface, the r's refracted angles, and the ψ's the angles which the surface tangents make with the vertical. The θ_b represents θ_{bulge}.

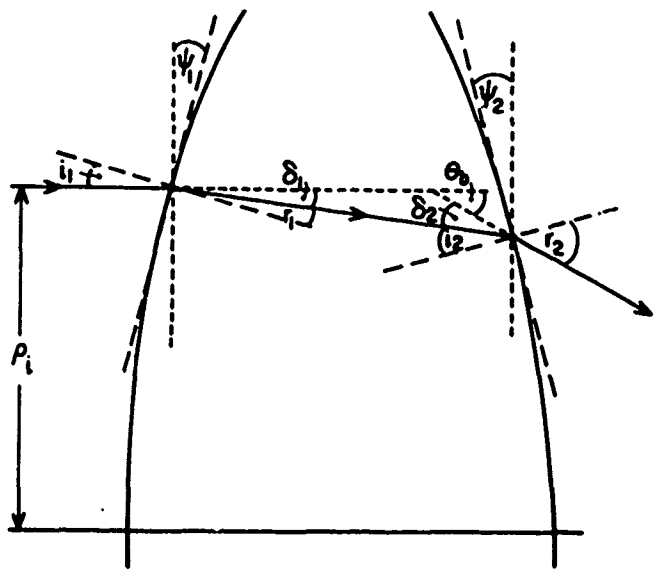

Figure C1. The Refraction of a Ray as It Passes Through a Bulging Window

From the inner triangle, we see that

$$\theta_b = \delta_1 + \delta_2 \qquad \text{(C-1)}$$

which can be replaced by:

$$\theta_b = (i_1 - r_1) + (r_2 - i_2) . \qquad \text{(C-2)}$$

Now, Snell's law at each interface is approximated by:

$$n \cong i_1/r_1 \cong r_2/i_2 . \qquad \text{(C-3)}$$

Substituting this information into (C-2), it becomes:

$$\theta_b = (n-1)\, r_1 + (n-1)\, i_2 . \qquad \text{(C-4)}$$

In the small angle-of-deviation approximation, however,

$$r_1 \approx \psi_1 = \left(\frac{dL}{d\rho}\right)_{\rho=\rho_i}$$

and

$$i_2 \approx \psi_2 \approx \psi_1 .$$

When these replacements are inserted into Eq. (C-4), the net result is:

$$\theta_{bulge} = 2(n-1)\left(\frac{dL}{d\rho}\right)_{\rho=\rho_i} . \qquad \text{(C-5)}$$

Appendix D

The Circle of Least Confusion From Geometric Optics

In this Appendix we calculate the radius of the circle of least confusion and its distance from the window using geometric optics for either polarization. We define the distance from the window to the point where the ray crosses the z axis by:

$$R(\rho) = \frac{\rho}{-\theta_{tot}} = \frac{\rho}{\gamma(\rho/\rho_o)} \tag{D-1}$$

where,

$$\gamma(\rho/\rho_o) \equiv -\theta_{tot}, \tag{D-2}$$

in the small angle-of-deviation approximation. Employing Eq. (51) in the above:

$$\gamma\left(\frac{\rho}{\rho_o}\right) = \frac{\rho_o}{R_o}\left(\frac{\rho}{\rho_o}\right) + F_1\left(\frac{\rho}{\rho_o}\right)\left[1 - F_2\left(\frac{\rho}{\rho_o}\right)^2\right], \tag{D-3}$$

and,

$$R(\rho) = \left\{\frac{1}{R_o} + \frac{F_1}{\rho_o}\left[1 - F_2\left(\frac{\rho}{\rho_o}\right)^2\right]\right\}^{-1}. \tag{D-4}$$

Since R_o is always in front of the window (i.e., positive), we will confine our attention only to those circumstances in which $R(\rho)$ also remains positive. Regardless of the magnitudes and signs of F_1 and F_2, this condition can always be satisfied provided $1 - F_2 (\rho/\rho_o)^2$ is always greater than $- \rho_o/F_1 R_o$. Then R, and hence θ_{tot}, remain monotonic with ρ.

In Figure 5, we depict two of the rays for the case in which R increases monotonically with ρ. The ray emanating from $\rho = \rho_o$ makes an angle of γ_o with the horizontal and has an equation given by:

$$\rho = - \gamma_o z + \rho_o . \tag{D-5}$$

A second ray, emanating from $\rho = -\rho'$, is shown coming from the bottom half of the window for reasons that will soon become obvious. It makes an angle of γ' with the horizontal so that its equation is:

$$\rho = \gamma' z - \rho' . \tag{D-6}$$

The two rays intersect at a distance r from the origin given by:

$$r = \frac{1}{\gamma_o + \gamma'} \left[\rho_o \gamma' - \rho' \gamma_o \right]. \tag{D-7}$$

The maximum value of r, which we call r_c, is the radius of the circle of least confusion. To obtain r_c, we first maximize r in Eq. (D-7) with respect to ρ'/ρ_o and get a corresponding value for ρ'. This particular ρ', together with ρ_o, are all that is necessary to prescribe those two rays which are sufficient to determine the circle of least confusion.

Taking the derivative of Eq. (D-7) with respect to ρ'/ρ_o results in:

$$\frac{dr}{d(\rho'/\rho_o)} = \rho_o(\gamma_o+\gamma') \left(\frac{d\gamma'}{d(\rho'/\rho_o)} - \gamma_o \right) - \rho_o \left(\gamma' - \frac{\rho'}{\rho_o} \gamma_o \right) \frac{d\gamma'}{d(\rho'/\rho_o)} . \tag{D-8}$$

Setting this equal to zero yields:

$$\left(\frac{\rho'}{\rho_o} + 1 \right) \frac{d\gamma'}{d(\rho'/\rho_o)} = \gamma' + \gamma_o . \tag{D-9}$$

Now utilizing Eq. (D-3) at both ρ_o and ρ', the above reduces to:

$$2\left(\frac{\rho'}{\rho_o}\right)^3 + 3\left(\frac{\rho'}{\rho_o}\right)^2 - 1 = 0 . \tag{D-10}$$

Of the three solutions, namely, 1/2, -1, and -1, only $\rho'/\rho_o = 1/2$ is the physically acceptable solution. Substituting this into (D-7) and changing r to r_c, the radius of the circle of least confusion, for either polarization, is now given as:

$$r_c^j = \frac{\rho_o}{4}\left\{\frac{F_1^j(t)\,F_2^j}{\frac{\rho_o}{R_o} + F_1^j(t)\,(1 - \frac{3}{4}F_2^j)}\right\}. \qquad \text{(D-11)}$$

The distance of the circle of least confusion from the window, D_c^j can be obtained from either Eqs. (D-5) or (D-6) if z is replaced by D_c^j and ρ by r_c^j. Solving for D_c^j results in:

$$D_c^j = \frac{\rho_o}{\frac{\rho_o}{R_o} + F_1^j\,(1-\frac{3}{4}F_2^j)}. \qquad \text{(D-12)}$$

When $R(\rho)$ is a monotonically decreasing function of ρ, we find that the same equations as given above hold and that r_c^j and D_c^j have the same forms as in Eqs. (D-11 and 12). The signs of the F- functions may differ, however, and only the magnitude of r_c^j is of consequence.